THE GLOBAL DISTRIBUTION OF PYROCLASTIC DEPOSITS ON MERCURY: THE VIEW FROM ORBIT. L. Kerber[1], S. Besse[2] J.W. Head[3], D.T. Blewett, T.A. Goudge [1]Laboratoire de Météorologie Dynamique, 4 Place Jussieu, Tours 55-66, Case Courrier 99, Paris, France (kerber@lmd.jussieu.fr), [2]European Space Research and Technology Center, Noordwijk, Netherlands, [3]Department of Geological Sciences, Brown University, Providence, RI 02912, USA, [4]Johns Hopkins University Applied Physics Laboratory, Laurel, MD 20723, USA.

Introduction: Pyroclastic volcanism was identified on Mercury from images acquired during three flybys by the MErcury Surface, Space ENvironment, GEochemistry, and Ranging (MESSENGER) spacecraft between 2009 and 2010 [1–5]. Approximately 40 candidate deposits were identified from flyby data, but it was hypothesized that a substantial number of deposits remained unidentified because of non-ideal viewing geometry and limited image resolution [5]. On 18 March 2011, MESSENGER was inserted into orbit around Mercury. Data from the orbital phase allows for greatly improved analysis of previously identified pyroclastic deposits and enables the identification of additional deposits [6–7].

Here we report the results of a global survey of pyroclastic deposits conducted using a combination of Mercury Dual Imaging System (MDIS) wide-angle camera (WAC) and narrow-angle camera (NAC) images. We document the locations of ~90 previously unidentified pyroclastic deposits, bringing the total number of candidate pyroclastic deposits to 137.

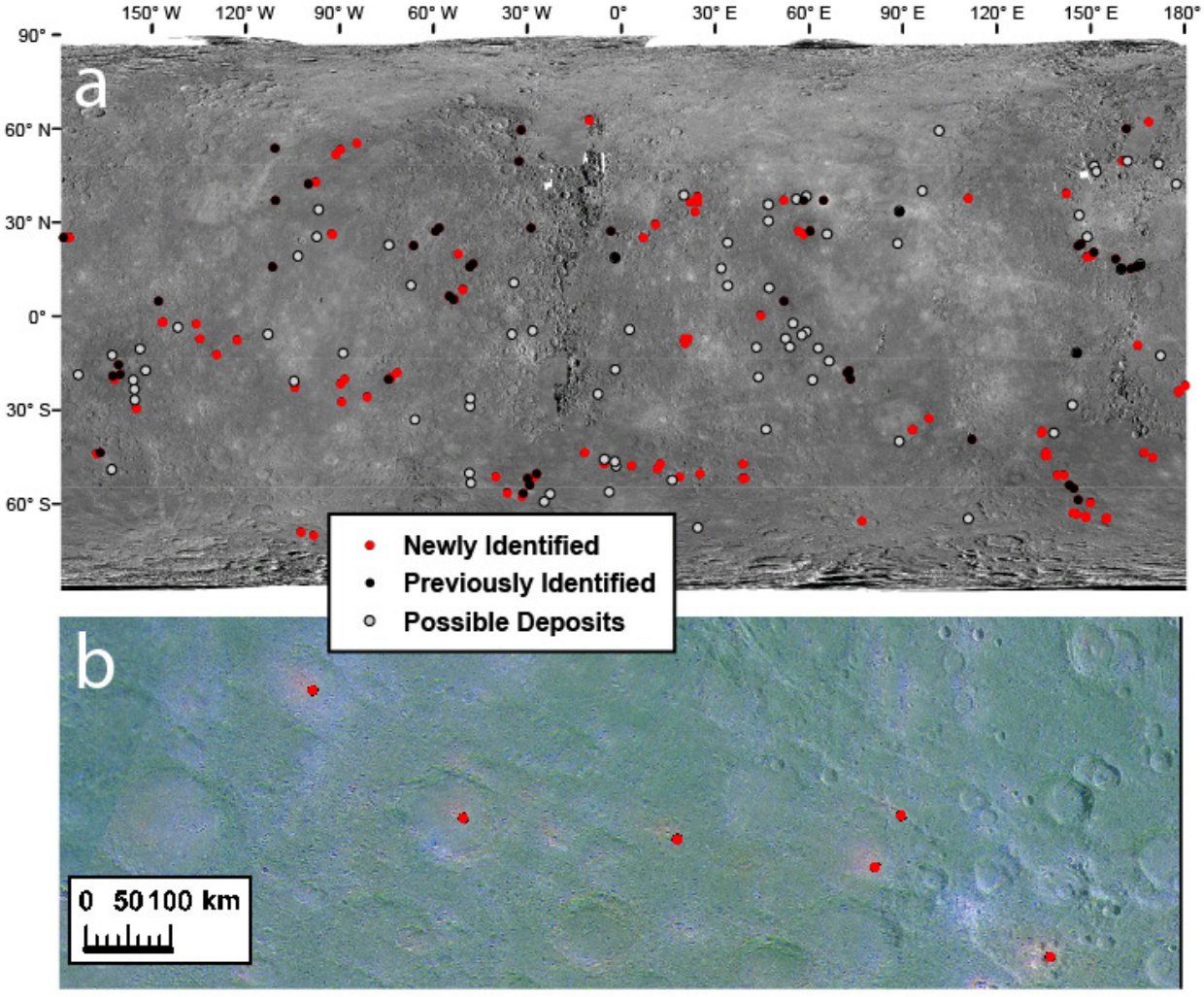

Figure 1. (a) Locations of newly identified pyroclastic deposits along with previously identified deposits. "Possible deposits" are those with a pyroclastic spectral signature but which either do not have an associated pit or for which insufficient data are available. (b) A portion of an RGB representation of spectral unmixing of an 8-band global WAC mosaic. Lat: -47°, Lon: 0° (R: Pyroclastic deposits, G: Exterior Caloris plains, B: Fresh craters). Pyroclastic deposits appear as orange spots.

Methods: This study made use of global WAC mosaics produced by the MESSENGER team for 8 WAC spectral bands (between 430 nm and 1000 nm). These products were processed using the software package ENVI. Five spectra were chosen that were representative of various common Mercurian materials (including interior Caloris plains, exterior Caloris plains, fresh crater rays, hollows, and pyroclastic material). Following earlier methods [5], the 8-band global scene was spectrally unmixed into these five composition types. In this manner several red-green-blue (RGB) composites could be made to reveal areas with spectral signatures similar to previously identified pyroclastic deposits. **Figure 1a** shows one of the RGB images produced using this technique. Rectilinear artifacts and abrupt changes in color are caused by uncorrected calibration differences between individual images making up the global mosaic, or by limitations of the photometric normalization. Despite these artifacts, the more consistently favorable illumination conditions provided by MESSENGER orbital data compared with the flyby data allow more robust identifications of pyroclastic deposits over most of the surface. Locations with an apparently pyroclastic signature were marked and examined in closer detail with both NAC and WAC images.

Results: Ninety previously unidentified pyroclastic deposits were mapped (red circles, **Figure 1b**). Many of the pyroclastic deposits identified are either smaller than those previously mapped or located in areas where the viewing geometry was not favorable during the flybys [5]. Gray circles indicate places where a pyroclastic-like spectral signature was apparent but a central, irregularly shaped pit was not obvious, either because it was not present or because the image resolution was not sufficient to identify it. In many of these cases the pyroclastic-like spectral signature was correlated with either crater central peaks or crater rims, usually where a slump had occurred. These locations could represent exposure of buried pyroclastic material by slumping or uplift during the cratering process, or it may be that this material is unrelated to pyroclastic processes and simply has similar WAC spectral characteristics. Very few pyroclastic deposits were found within the northern plains.

Three different types of pyroclastic landforms were observed. The most common consist of deep, irregular, elongate pits or series of pits (**Fig. 2b**). These range in morphology from large, arcuate pits with rounded edges to small, oval pits with pinched ends and sharp cliffs. The second type consists of shallow, scabby pits (**Fig. 2a**, black arrows), morphologically more similar to hollowed terrain [8-9] (white arrows), though at a much larger scale. The third type (for which there exist only three examples) consists of a raised mound or cone, much larger than a normal crater central peak. These could be volcanic constructs, which appear to be rare on Mercury (**Fig. 2c-e**).

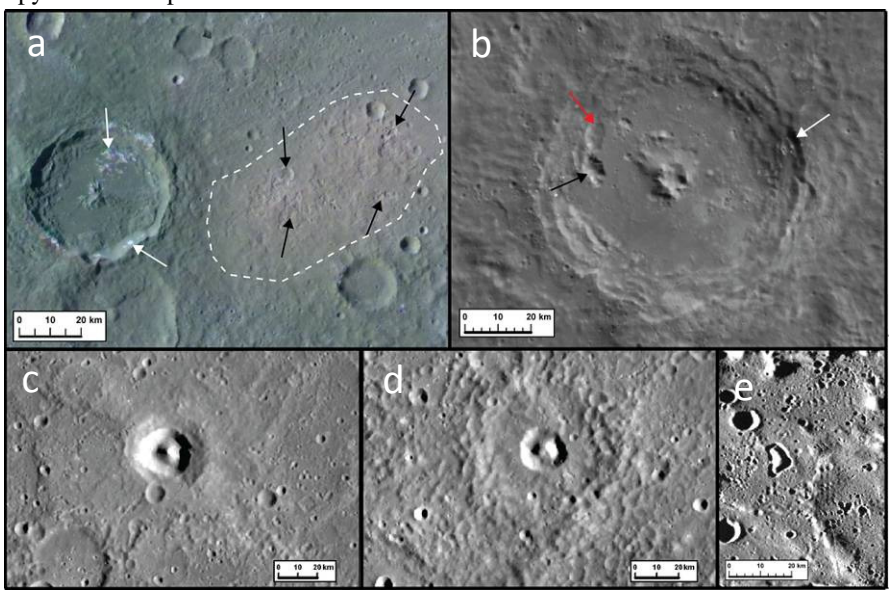

Figure 2. (a) Shallow, scab-like pyroclastic pits (black arrows) next to hollows (white arrows). (b) Elongated pits of varying freshness (black and red arrows) and an unusual dark deposit (white arrow). (c-e) Positive features (mounds and cones) with pyroclastic-like spectral signatures.

Acknowledgments: We thank Nancy Chabot and the MESSENGER team for making available the MDIS global color mosaics that made this analysis possible.

References: [1] Head, J.W. et al. (2008) *Science 321*, 69-72. [2] Kerber, L. et al. (2009) *EPSL 285*, 263-271. [3] Blewett, D.T. et al. (2009) *EPSL 285*, 1245-1254. [4] Head, J.W. et al. (2009) *EPSL 285*, 227-242. [5] Kerber, L. et al. (2011) *PSS 59*, 1895-1909 [6] Goudge, T.A. et al. (2013) *JGR Planets*, submitted. [7] Rothery, D. et al. (2014) EPSL 385, 59-67. [8] Blewett, D.T. et al. (2013) *JGR Planets 118*, 1013-1032. [9] Thomas, R.J. et al. (2014) *Icarus 229*, 221-235.